Published in final edited form as:
Oncogene. 2009 October 8; 28(40): 3513–3525. doi:10.1038/onc.2009.220.

Sonic Hedgehog Paracrine Signaling Regulates Metastasis and Lymphangiogenesis in Pancreatic Cancer

Jennifer M. Bailey[1], **Ashley M. Mohr**[1], and **Michael A. Hollingsworth**[1,2,5]
[1]Eppley Institute, University of Nebraska Medical Center. Omaha, NE 68198-6805

Abstract

Sonic hedgehog (SHH) expression is tightly regulated throughout development. In the adult, aberrant expression of SHH is associated with the onset and progression of pancreatic cancer, as evidenced by increased levels of expression in premalignant and malignant lesions of the pancreas. We investigated the hypothesis that SHH, secreted from pancreatic tumors, functions in a paracrine manner to influence the biological condition of mesenchymal and endothelial cells. Orthotopic implantation of a pancreatic tumor cell line expressing SHH (Capan-2) and a transformed primary cell line that overexpresses SHH (T-HPNE.SHH) were used to show that overexpression of SHH increased primary tumor size and metastasis. Treatment with a neutralizing antibody, 5E1, decreased primary tumor volume and inhibited metastasis. Lyve-1+ vessels and stromal fibroblasts in tumors expressed primary cilium and showed localization of the receptor Smoothened to the primary cilium, providing evidence of active SHH signaling through this pathway. While primary cilia are present on normal ductal cells of the pancreas, we did not observe primary cilium on the ductal tumor cells, suggesting decreased autocrine signaling through pathways mediated by the primary cilium in pancreatic cancer. These data support the hypothesis that SHH, secreted from pancreatic epithelia, is a critical player in establishing and regulating the tumor microenvironment and thereby contributes to progression of pancreatic cancer.

Keywords

Pancreatic Cancer; Sonic Hedgehog; Lymphangiogenesis; metastasis

Introduction

Sonic Hedgehog (SHH), known for influencing tissue patterning in developing embryos (Ingham and McMahon, 2001; McMahon *et al.*, 2003; Odent *et al.*, 1999; Villavicencio *et al.*, 2000), is a secreted morphogenic signaling protein that functions by binding to a 12-pass transmembrane protein called Patched (Ptch) (Marigo *et al.*, 1996). SHH binding to Ptch releases the inhibitory affects of Ptch on a serpentine protein, Smoothened (SMO), which activates other downstream effectors that culminate with nuclear localization of the Gli2 transcription factor and upregulation of target genes, including Ptch, Gli1 and Hhip (Lipinski *et al.*, 2006; Murone *et al.*, 1999). Mutations in the hedgehog pathway and aberrant expression of SHH are found in cancers (reviewed in (Pasca di Magliano and Hebrok, 2003)).

[2]Corresponding Author: Dr. M.A. Hollingsworth Eppley Institute for Research in Cancer and Allied Disease University of Nebraska Medical Center 986805 Nebraska Medical Center Omaha, NE 68198-6805 Phone: (402) 559-8343 Fax: (402) 559-4651 mahollin@unmc.edu. [5] To whom reprint requests should be addressed..

The hedgehog signaling complex has been shown to organize and conduct signal transduction events at the primary cilium (Corbit *et al.*, 2005; Rohatgi *et al.*, 2007). Primary cilia are microtubule-based organelles that protrude from the centriole to the extracellular environment of quiescent cells. In human pancreatic epithelial cells, loss of primary cilia function is associated with an increase in the formation of cysts and lesions associated with pancreatitis or cystic fibrosis (Cano *et al.*, 2006). The mechanisms by which primary cilia regulate hedgehog signaling in pancreatic cancer remain to be explored.

Pancreatic Ductal Adenocarcinoma (PDAC) is a lethal disease with a death to incidence ratio of 0.99 (Jemal *et al.*, 2004), whose genesis and progression is poorly understood. SHH is not expressed in the normal adult pancreas but is expressed in premalignant (PanIN) and ductal adenocarcinoma cells of pancreatic origin (Thayer *et al.*, 2003). Initial studies into the role of SHH in the initiation and progression of pancreatic cancer have shown only modest direct autocrine effects on tumor progression (Liu *et al.*, 2007; Morton *et al.*, 2007; Thayer *et al.*, 2003). Aberrant expression of SHH in the developing murine pancreas induces metaplasia but does not lead to adenocarcinomas that are typical of human disease (Kawahira *et al.*, 2005; Kayed *et al.*, 2006). We sought to explore the contribution of SHH to pancreatic cancer initiation, progression, angiogenesis and tumor growth. We expressed SHH in a transformed ductal-derived epithelial cell line from the human pancreas that was immortalized with the catalytic subunit of telomerase (hTert-HPNE) (Lee *et al.*, 2003) and transformed by sequential transduction with retroviral vectors that provide oncogenic insults that mimic the current progression model of pancreatic cancer (the transformed cell line is called T-HPNE). The results showed that SHH had only subtle autocrine effects on transformed cells *in vitro,* but *in vivo* enhanced angiogenesis and regulated angiogenesis. Furthermore, blocking SHH activity with a specific antibody inhibited tumor growth, lymphangiogenesis and metastasis. The results provide additional evidence that SHH is a regulator of the tumor microenvironment and thereby contributes to progression of pancreatic cancer.

Materials and Methods

Cell lines, culture conditions

The hTert-HPNE cells were originally isolated from the ductal structure of a human pancreas and were immortalized with the catalytic subunit of telomerase (h-Tert), along with subsequent transductions to introduce a Kras mutation, the human papillomavirus E6 and E7 peptides and the SV40 small t antigen, as was described previously (Lee *et al.*, 2003). The hTert-HPNE cells were maintained in Medium D containing one volume of M3 base (InCell Corp., San Antonio, TX, USA), three volumes of glucose-free DMEM, 5% FBS, 5.5mM glucose, 10ng/ml EGF, and 50μg/ml gentamycin, at 37°C in humidified atmosphere containing 5% CO_2.

Capan-2 cells are maintained in McCoy's 5A with 10% FBS at 37°C in humidified atmosphere containing 5% CO_2.

HMVEC-dLy (Clonetics Dermal Lymphatic Microvascular Endothelial Cell Systems were maintained in EGM-2 complete media at 37°C in humidified atmosphere containing 5% CO_2.

Primary Cell Culture

Primary human pancreatic fibroblasts were isolated from human pancreatic tissue, as was described previously (Lee *et al.*, 2003). Cells were monitored for several weeks and were identified by cellular morphology and staining of markers as cells of mesenchymal, stellate or epithelial lineage.

Western Blot Analysis and Reagents

Whole cell lysates were prepared by adding 1.5 ml NP40 cell lysis buffer [10 nmol/L Tris-HCl (pH 8.0), 150mmol/L NaCl, 1 mmol/L phenylmethylsulfonyl fluoride and 1% Triton X-100] to cells grown to 80% confluence in T175 tissue culture flasks. Sixty micrograms of protein were loaded onto 4-20% Novex Tris-Glycine gradient denaturing polyacrylamide gels (Invitrogen) in a 1x SDS-PAGE running buffer, containing 1g/L SDS, 3g/L Tris base, and 14.4 g/L glycine. The proteins were transferred onto polyvinylpyrolidine diflouride membranes by electrophoresis. Once transferred, the membranes were blocked in Blotto [5% dry milk resuspended in 1x TBS (0.9% NaCl, 10mmol/L Tris pH 7.4, and 0.5%MgCl)] overnight at 4°C. Anti-SHH primary antibody (Santa Cruz, CA, USA) was incubated at a 1:200 dilution at room temperature for 2 hours. The membrane was washed 3 times, 10 minutes each time, before the addition of the secondary antibody (goat anti-rabbit HRP) at a dilution for 50 minutes.

For analysis of EMT, the cells were washed with 1X PBS and proteins were extracted using radioimmunoprecipitation assay buffer. 80ug of protein were loaded per well. For protein analysis: vimentin is from Chemicon (Temecula, CA) fibronectin is from abcam (Cambridge, MA), the mouse monoclonal against E-cadherin was a gift from M. Wheelock (Omaha, NE) and has been described (Peralta Soler *et al.*, 1995). The mouse monoclonal against N-cadherin was also a gift from M. Wheelock and has been described (Peralta Soler *et al.*, 1995; Wahl *et al.*, 2003). Other antibodies included HIF1α (abcam 1:400), VEGF (Santa Cruz 1:200), ph-AKT/AKT, ph-ERK/ERK (1:1000 Cell Signaling), MMP9 (Neomarkers 1:200), Patched and Gli3 (Santa Cruz 1:100). For all blots, complexes were identified using ECL Western blotting detection reagents. Membranes were stripped at subsequently blotted with anti β-actin antibody as a loading control.

Cell Proliferation Assay

T-HPNE and T-HPNE.SHH cells were plated (in triplicate for each experiment) in 96 well plates at a density of 2,000 cells/ well. The cells were monitored for viability using MTT reagent at 24 and 96 hours. At the given time points, MTT reagent was added to the media and allowed to incubate for 4 hours at 37° C in a humidified incubator at 5% CO_2. The grains were then attached to the bottom of the plate by centrifugation and DMSO was added to dissolve the grains. Cell viability was quantified by reading the plates at an absorbance of 570 nm.

Colony Forming Assay

NuSieve GTR low melting agarose FMC Bioproduct #50082 was used in this experiment to create a 0.6% bottom agar solution and a 0.4% top agar solution. HPNE cells were mixed in the top agar solution before the agar was allowed to solidify at a density of 50,000 cells per 6-well plate. The cells were allowed to incubate at 37° C for 10 days before being stained with crystal violet and counted.

Matirgel Invasion Assays

In vitro invasive potential of cells overexpressing SHH was assayed using the Biocoat Matrigel Invasion Chamber (Becton Dickinson Labware, Bedford, MA). T-HPNE and T-HPNE.SHH were seeded onto the upper chamber of double-structured matrix gel chamber at a density of 1×10^5 cells/ chamber. The cells in the upper chamber were seeded in serum-free Medium D. The lower chamber contained Medium D with the addition of 10% FBS. The chambers were cultured at 37°C for 22 hours in a humidified incubator containing 5% CO_2. For analyses of all invasion assays, cells on the upper portion of the matrix membrane were wiped off with cotton tipped swab and cells on the bottom of this membrane were fixed and

stained with Diff-Quick staining kit (Allegiance) and observed by a light microscopy. The number of invading cells was quantified by counting the membranes at 200X magnification. **For migration assays**, 5,000 HMVECs were seeded into the upper chamber of a Biocoat Matrigel Invasion Chamber-using the control insert alone to analyze migration. The cells were seeded in complete media in the upper chamber and were stimulated by the addition of rhSHH at 1.0μg/ml, 5.0μg/ml or 10.0μg/ml and analyzed after 22 hours, as described previously.

Stimulation of Pancreatic Fibroblasts with SHH

Cells were seeded in T75 flasks and were serum starved for 16 hours. Cells were then stimulated with recombinant human SHH (rhSHH from R&D Systems) at three concentrations: 0.1μg/ml, 1.0μg/ml and 5.0 μg/ml. The cells were stimulated for 24 hours before lysates were taken.

Subcutaneous Injections in Athymic Nude Mice

Three million cells were injected in a subcutaneous model in athymic nude mice. Prior to injection, the cells were trypsinized, counted, washed twice in 1xPBS and resuspended at a density of 3×10^6 cells/ 30μl, and injected between the scapulae. Tumor growth was monitored every two days, by calculating diameter in two dimensions using a caliper. The mice were euthanized when the tumor volume reached 1,800mm^3. For co-injection experiments, 1×10^6 cells/ 30μl + 10,000 fibroblasts or 1.11^6 cells/ 30μl (tumor cells only) were injected between the scapulae.

Orthotopic implantation in athymic nude mice

One million T-HPNE and T-HPNE.SHH were each injected into the pancreas of 12 or 13 mice to analyze tumor growth, metastases and desmoplasia in response to overexpression of SHH. Preparation of cells was described in the subcutaneous injection model. Orthotopic implantation of HPNE cell lines was done, as was described previously (Tsutsumida *et al.*, 2006). In another set of experiments, one million Capan-2 cells were implanted into the pancreas of athymic nude mice. One group of mice were controls, one group was given 500ug of 5E1 (Pepinsky *et al.*, 2000) once each 7 days and the last group was administered an IgG control antibody (4EII) at the same dose as 5E1.

Immunohistochemical and Confocal Analysis

To identify SHH in the primary and metastatic human tumor sections, SHH (1:200) (Santa Cruz, CA, USA) anti-rabbit primary antibody (Santa Cruz, CA, USA) was incubated on paraffin-embedded tissue sections for 2 hours at 37° C. The secondary staining was identified by Vectastain ABC reagent and DAB substrate. For confocal analysis, SHH (Santa Cruz 1:200), anti acetylated a-tubulin from Sigma (1:500), Smo (Santa Cruz 1:100), Lyve-1 (abcam 1:100). Secondary fluorescent probes are from Invitrogen (Eugene, OR): (anti-rabbit IgG alexa flour 594 and anti-mouse IgG alexa flour 647, anti-goat IgG alexa flour 488).

In vitro angiogenesis assay

In vitro angiogenesis assays were performed using the angiogenesis kit from Chemicon, ECM625. The HMVECs were seeded at a density of 10,000 cells per well in a 96-well plate. Complete media alone, or with rhSHH or rhSHH+5E1 were the treatment groups. The cells were monitored once every two hours for 8 hours. The notation of results is described by the following numerical designation: (1) cells begin to migrate and align; (2) capillary tubes visible; (3) sprouting of new capillary tubes; (4) closed polygons form and (5) complex mesh structures develop, as described in the data sheet for the assay.

Annexin V & Propidium Iodide Staining

The cells were trypsinized, pelleted, washed with 1X PBS, and resuspended in 1X Annexin V binding solution (BD Biosciences). 10 ul of Annexin V-FITC and 2ug of Propidium Iodide were added to the cells and allowed to incubate for 30 minutes at 4°C. 400ul of Annexin V binding solution was then added and the cells were analyzed by flow.

Statistical analysis

The *in vitro* colony forming assays and invasion assays were analyzed using a one-way Anova test and were graphed using Prizm statistical analysis. Motility assays were analyzed using a two-way Anova using Prizm. Significance was determined at the 95% confidence interval. Failure-free survival (FFS) was used to analyze the time to tumor progression in the subcutaneous model of tumor growth and progression. FFS was defined as the onset of tumor formation, enabling a calculation for percent disease-free mice relative to time. Estimates of time to tumor formation were calculated using the Kaplan and Meier method and outcomes were analyzed using a log-rank test. To compare the incidence of metastasis in the orthotopic model, a Fisher's exact test was used to compare cell lines, while a Mann-Whitney test was used to calculate any significant difference in the weight of the primary tumors.

Results

SHH overexpression promotes tumor growth and metastasis

The activity of SHH on the transformed growth properties of the T-HPNE and T-HPNE.SHH cell lines was evaluated *in vivo* by measuring tumor growth following subcutaneous injection of 3 million cells into athymic mice. SHH overexpression significantly decreased time to tumor progression for the T-HPNE.SHH cell line to 11 days versus 27 days for the T-HPNE cell line (Figure 1A). SHH expression did not affect tumor growth rate in the subcutaneous model once the tumors had appeared (Figure 1B).

The SHH overexpression model was further investigated in an orthotopic tumor model, where one million cells of the T-HPNE and T-HPNE.SHH cell lines were implanted into the pancreas of athymic mice. Mice were sacrificed at 46 days post tumor challenge. SHH expression in the orthotopic tumors was confirmed by western blot analysis (Figure 1C). Similar to findings in the subcutaneous model, SHH overexpression in the T-HPNE cell line resulted in significantly increased weights of primary tumors (Figure 1D). Moreover, tumors expressing SHH had increased incidence of tumor invasion and metastasis to the spleen, peritoneum and liver (Figure 1E). Hedgehog signaling pathways are known regulators of angiogenesis in cancer and development (Nagase *et al.*, 2008; Straface *et al.*, 2008; Velcheti, 2007). Immunohistochemical analysis of the orthotopic tumor sections for CD31 was used to determine if overexpression of the SHH ligand contributed to angiogenesis. The orthotopic tumors derived from the T-HPNE.SHH cell line showed increased microvessel density as evidenced by staining for CD31 (Figure 1F).

SHH expression in T-HPNE cells enhances transformed growth properties *in vitro*

We sought to determine the relative contribution of autocrine SHH stimulation to growth of the T-HPNE and T-HPNE.SHH cells. Previous publications have shown that cyclopamine treatment of pancreatic cancer cells lines resulted in reduced growth rates and increased rates of apoptosis (Thayer *et al.*, 2003). SHH expression did not significantly increase the growth rate of the T-HPNE cell line *in vitro* (data not shown). Consistent with previous reports that SHH regulates epithelial-to-mesenchymal changes (Feldmann *et al.*, 2007), we detected moderate epithelial-to-mesenchymal (EMT) changes in the T-HPNE.SHH as evidenced by an increase in vimentin and a loss of E-cadherin by western blot analysis. SHH

expression significantly increased *in vitro* invasion on Matrigel-containing chambers (Supplemental Figure 1).

Isolated populations of pancreatic cancer stem cells (or tumor initiating cells) have been shown to express SHH (Li *et al.*, 2007). Therefore, we investigated the effect of SHH expression on the percentage of putative cancer stem cells expressing CD133, a marker associated with stem cells/tumor initiating cells in pancreatic cancer if not all cancers (Heeschen, 2008; Hermann *et al.*, 2007)). SHH expression in the T-HPNE cells increased the percentage of CD133+ putative cancer stem cells as compared to controls (Supplemental Figure 1).

SHH paracrine signaling enhances tumor formation *in vivo*

We previously published that SHH expression in tumor cells regulates the desmoplastic response in pancreatic cancer (Bailey *et al.*, 2008). This, together with observations that SHH expression by T-HPNE cells did not enhance cell growth rates *in vitro*, but decreased time-to-tumor progression and increased angiogenesis *in vivo*, led us to hypothesize that the effects on tumor growth were the result of paracrine signaling by SHH to stromal cells, including fibroblasts. To test this hypothesis, we co-injected 10,000 human pancreatic fibroblasts mixed with 1×10^6 T-HPNE or T-HPNE.SHH cells and evaluated tumor growth properties *in vivo*. Figure 2A shows results of this experiment in terms of % disease-free mice over time. Co-injection of human pancreatic fibroblasts resulted in a significant decrease in time-to-tumor progression when comparing T-HPNE.SHH cells alone to T-HPNE.SHH cells that were co-injected with pancreatic fibroblasts. Moreover, there was no difference in time-to-tumor progression when T-HPNE cells not expressing high levels of SHH were co-injected with human pancreatic fibroblasts (Figure 2A).

Histological examination of cross-sections of tumors showed an obvious increase in the number of blood vessels in the T-HPNE.SHH cells co-cultured with the human pancreatic fibroblasts when compared to the T-HPNE.SHH cells alone (Figure 2B and C). These data suggest that the interactions between SHH, secreted from the tumor cells, and fibroblasts in the tumor microenvironment increase angiogenesis and tumor progression in pancreatic cancer.

Tumor-associated stromal cells express a primary cilium

Recent publications have emphasized the significance of the primary cilium to initiate cellular responses to SHH ligand stimulation through Patched and Smoothened (Corbit *et al.*, 2005; Rohatgi *et al.*, 2007). We sought to evaluate the role of SHH signaling that is mediated by the primary cilium. We evaluated human primary pancreatic tumors and liver metastases for the presence of primary cilium, and looked for evidence of SHH signaling complexes at primary cilia by the co-localization of SMO. Consistent with recent work on the localization of primary cilia in the developing pancreas (Nielsen *et al.*, 2008) and previous work citing expression of primary cilia in the islets and ductal cells, but not the acini (Cano *et al.*, 2004; Cano *et al.*, 2006; Zhang *et al.*, 2005), we observed staining for primary cilium in normal pancreatic ducts, but did not detect staining in acinar cells (Figure 3A). We did not detect staining for the receptor SMO in either the ductal and acinar cells. In contrast, as shown in Figure 3B, we observed that primary were cilium localized to the stroma, but were absent on tumor cells from primary pancreatic tumors, which instead produced SHH. Notably, we observed localization of the receptor SMO along primary cilia in the stroma surrounding the tumor cells (Figure 3C), confirming the potential for SHH pathway activation in the local tumor microenvironment. We also evaluated expression of SHH, SMO and the primary cilium in liver metastases of pancreatic tumors (Figure 3D). Confocal analysis showed that metastatic pancreatic ductal adenocarcinoma cells expressed

SHH, but showed no staining for the primary cilium marker, acetylated α tubulin (acet. tub.), and also lacked staining for SMO. In contrast, stromal cells adjacent to the SHH-expressing metastatic duct expressed abundant primary cilium and showed localization of the receptor SMO to the primary cilium. Notably, the stromal cells expressed very high levels of SMO as compared to the tumor cells.

SHH paracrine signaling in human pancreatic fibroblasts

The observation of increased angiogenesis in the T-HPNE.SHH tumors led us to examine expression of the pro-angiogenic cytokine Vascular Endothelial Growth Factor (VEGF) and HIF1α. Previous reports have implicated cross-talk between SHH and HIF1α (Hwang *et al.*, 2008). We used immunohistochemistry to evaluate expression of VEGF and HIF1α in tumor sections derived from the T-HPNE.SHH cells. We detected increased stabilization of HIF1α, a know regulator of VEGF expression and a published indicator of poor prognosis in patients with pancreatic cancer (Hoffmann *et al.*, 2008). We examined the cell source of HIF1α in these tumors by using IHC. Smooth muscle actin + fibroblasts in the T-HPNE.SHH tumor sections showed increased staining for HIF1α and also expressed Gli 1 (Figure 4A and B), indicating that these cells were responsive to paracrine stimulation with SHH. The tumor-associated fibroblasts also stained positive for the expression of VEGF (Figure 4A and B).

These observations led us to determine if SHH ligand stimulation of pancreatic fibroblasts *in vitro* increased expression of VEGF. SHH pathway activation was confirmed by analysis of SHH-stimulated pancreatic fibroblasts, which showed increased expression of the receptor Patched and increased cytoplasmic expression of the transcriptional repressor, Gli3 (Figure 4C). Figure 4C also presents a western blot analysis showing that stimulation of human adult pancreatic fibroblasts with SHH increased the expression of VEGF.

We sought to determine how SHH was regulating the expression of VEGF. We hypothesized that SHH stabilizes HIF1α under normoxic conditions in human pancreatic fibroblasts. Figure 4D presents western blot analysis of human pancreatic fibroblasts stimulated with SHH in the presence of the proteosome inhibitor MG132 under normoxic conditions. At a concentration of 5μg/ml, SHH stabilized levels of HIF1α. Examination of the expression of different metalloproteases in response to SHH in the pancreatic fibroblasts showed no increase in MMP 1 or MMP 7 (data not shown), but there was an increase in the expression of MMP 9 (Figure 4E). MMP 9 is a published target of Gli1 and a known regulator of metastasis and angiogenesis in pancreatic cancer (Nagai *et al.*, 2008). These data suggest that SHH-mediated paracrine signaling in fibroblasts in the tumor microenvironment enhances the expression of known regulators of angiogenesis and metastasis.

Treatment with a neutralizing antibody to SHH (5E1) significantly reduces tumor growth and metastasis

We investigated further the effect of neutralization of SHH on *in vivo* growth properties of pancreatic cancer cells. The moderately-differentiated human pancreatic cancer cell line, Capan-2, was orthotopically implanted into the pancreas of nude mice, which were subsequently treated weekly with a neutralizing antibody for SHH. The mice were monitored for 3 months and were sacrificed upon signs of cachexia. Figure 5A shows graphical representation of the average tumor volumes for mice that were not treated with any antibody, mice that were treated with an isotype IgG-control antibody (4E11), or mice treated with the SHH-neutralizing antibody (5E1). There was a significant decrease in tumor volume in mice treated with a neutralizing antibody against SHH.

Figure 5B presents a graphical representation of the percentage of mice with metastasis to different organ sites. Neutralization of SHH decreased metastatic disease in the liver, peritoneum and significantly decreased the number of mice with metastatic lymph nodes. We examined that possibility that neutralizing SHH induced apoptosis of the tumor cells by determining the number of caspase 3 + cells as a function of tumor volume. Treatment with 5E1 increased the number of caspase 3 + cells as a function of tumor volume (Figure 5C). *In vitro* treatment of Capan-2 cells with 5E1 did not induce apoptosis or significantly affect the proliferation rate of Capan-2 cells (Figure 5 D-F), suggesting that downstream affects of SHH paracrine signaling in the context of the tumor microenvironment are regulating cell survival during tumor growth *in vivo*.

Tumor-derived SHH paracrine signaling promotes lymphangiogenesis *in vitro* and *in vivo*

We observed significant decreases in the number of mice with metastatic lymph nodes when we administered the SHH neutralizing antibody (5E1). We therefore evaluated the effects of SHH on intratumoral lymphangiogenesis. Control and 5E1-treated Capan-2 tumors were evaluated for expression of two lymphatic markers, Lyve-1 and Podoplanin. The neutralization of SHH decreased the number of Podoplanin+ (Figure 6A) and Lyve-1+ (Figure 6B) cell types in the Capan-2 tumor sections. The number of Lyve-1+ vessels were significantly decreased in tumors from animals treated with 5E1 (Figure 6C). We further analyzed the affects of SHH paracrine signaling *in vitro* by stimulating a normal human lymphatic endothelial cell line (HMVEC) with recombinant human SHH. Stimulation with SHH significantly increased *in vitro* lymphangiogenesis (Figure 6D) and HMVEC motility (Figure 6E).

To confirm that tumor-derived SHH had the potential to signal through a paracrine mechanism to the lymphatic endothelial cells, we used confocal microscopy to determine if Lyve-1 + cells in the untreated Capan-2 orthotopic tumors expressed primary cilium and showed localization of the receptor SMO to the primary cilium. Figure 7A presents evidence that the Lyve-1+ cells expressed a primary cilium and showed localization of SMO to the primary cilium in a number of Lyve-1+ cells. We further analyzed the expression of the primary cilium on Lyve-1+ vessels in tissue sections from patients with pancreatic cancer that are confirmed to express SHH (note Figure 3). Figure 7B shows that isolated Lyve-1+ cells in primary tumors (**7B**) and liver metastasis (**7C**) express primary cilium and SMO is localized to the cilium in these cells.

Discussion

SHH is expressed in premalignant and malignant ductal epithelial cells of the pancreas, implicating this morphogenic signaling protein in the initiation and progression of pancreatic cancer. The data presented here and other reports (Morton *et al.*, 2007; Pasca di Magliano *et al.*, 2006) implicate SHH in tumor progression. Consistent with recent published data (Tian *et al.*, 2009; Yauch *et al.*, 2008), we suggest that paracrine signaling in stromal cells is critical to SHH-mediated effects on progression of pancreatic cancer. A previous publication from our laboratory implicated SHH as a regulator of the tumor microenvironment through the production of desmoplasia (Bailey *et al.*, 2008). The results presented previously and here are consistent with the concept that SHH functions as a morphogen in developing tissues, in which it has multiple and different effects on different cell types, and suggests that pancreatic tumors have appropriated this normal function in a manner that enables angiogenesis and metastasis by the production of pro-angiogenic and metastasis promoting effects in the stroma. These processes contribute significantly to disease progression to a metastatic phenotype, which is the major factor leading to the demise of the patient. Our results and other recent reports (Feldmann *et al.*, 2007) have confirmed that SHH contributes to the metastatic potential of pancreatic cancer, and in particular we show here that effects

on lymphangiogenesis are important and may influence the metastatic capacity of pancreatic tumors to lymph nodes.

The results presented here provide insight into both the autocrine and paracrine mechanisms by which SHH acts. With respect to autocrine effects, the most notable direct effect of SHH on T-HPNE cells was to enhance invasion *in vitro*, in part by inducing loss of E-cadherin in the T-HPNE.SHH cell line. These results are consistent with the hypothesis that SHH induces EMT in these cells, which is also consistent with its known effects in both normal (Apelqvist *et al.*, 1997; Kawahira *et al.*, 2005) and transformed cell types (Lee *et al.*, 2003). Other autocrine effects on transformed properties of tumor cells (proliferation, apoptosis) were minimal, except perhaps the observed increase in the percentage of CD133+ cells in culture, which may indicate that SHH serves to enhance the number of tumor initiating/stem cells. Moreover, the observed effects on EMT and invasion in the T-HPNE.SHH cell line suggests this small population of tumor-initiating cells may be more responsive to autocrine stimulation *in vitro* and *in vivo*.

Regarding paracrine mechanisms of action of SHH, our results are consistent with other recent findings, which show that SHH paracrine signaling is required for tumor progression (Tian *et al.*, 2009; Yauch *et al.*, 2008). It was notable that in primary tumor sections expressing SHH we observed stromal cells that showed localization of SMO to primary cilia, and saw evidence of active SHH signaling in this compartment (expression of Gli1). Primary cilia were not observed in tumor cells. This suggests that signaling downstream of SHH stimulation is different in tumor cells (autocrine) and stromal cells (paracrine). Specifically, our results suggest that SHH induced paracrine signaling through complexes at primary cilium induce molecular alterations in the stroma that promote angiogenesis, lymphangiogenesis and metastasis. These findings are important to both understanding the role of SHH in tumor progression, and to current efforts to regulate the effects of SHH through the use of small molecule inhibitors of events downstream of SHH stimulation. That there are different signaling mechanisms operative in tumor (not mediated by primary cilium) and stroma (mediated by primary cilium) suggest that more comprehensive strategies may be required to accurately modulate the overall effects of SHH on tumor progression. Inhibiting signaling that is specific for tumor cells may not influence different mechanisms of signaling that are operative in stroma, which our data suggest contribute substantially to tumor progression. Moreover, targeting the stroma of tumors such as pancreatic cancer may be very important for achieving other positive effects on treatment, such as improving drug delivery and influencing angiogenesis and lymphangiogenesis.

Our use of 5E1 to treat pancreatic tumor growth is unique, as other studies have largely used cyclopamine or other small molecule inhibitors (Feldmann *et al.*, 2007; Thayer *et al.*, 2003). Our findings that blocking SHH binding directly by antibody treatment causes dramatic effects on tumor growth and metastasis suggests that this strategy may be more effective in cases where SHH activates different downstream signaling pathways in different cells types, especially given that the specificity and activity of inhibitors such as cyclopamine are not well characterized.

In conclusion, SHH significantly affects the microenvironment and time-to-tumor progression in both subcutaneous and orthotopic mouse models of pancreatic cancer through paracrine effects. Our results suggest that SHH is a critical player in the tumor microenvironment, and that its further investigation is required to better understand the potential for SHH as a therapeutic target for diminishing the desmoplastic response and pathogenesis of metastatic pancreatic cancer.

Supplementary Material

Refer to Web version on PubMed Central for supplementary material.

Acknowledgments

We thank Dr. Kim McDermott for insight, comments and suggestions. We thank Dr. Rick Tempero and Dr. Phil Kelley for the gift of HMVEC cells and suggestions related to their use.

This work was supported by grants from the National Institutes of Health (R01CA57362, P30CA36727, U01CA111294), training grant awards to JMB and AMM (CA09476), and assistantship awards from the University of Nebraska (JMB)

Abbreviations used in this paper

HPNE	Human Pancreatic Nestin-Expressing Cells
hTert	catalytic subunit of human telomerase used to immortalize HPNE cells
T-HPNE	transformed HPNE cell line
T-HPNE+SHH	transformed HPNE cell line expressing Sonic Hedgehog
SHH	Sonic Hedgehog
MTT	(3-(4,5-dimethylthiazolyly-2)-2, 5-diphenyltetrazolium bromide)
Ptch	Patched
Smo	Smoothened
Hhip	Hedgehhog-interacting protein

References

Apelqvist A, Ahlgren U, Edlund H. Sonic hedgehog directs specialised mesoderm differentiation in the intestine and pancreas. Curr Biol 1997;7:801–4. [PubMed: 9368764]

Bailey JM, Swanson BJ, Hamada T, Eggers JP, Singh PK, Caffery T, et al. Sonic hedgehog promotes desmoplasia in pancreatic cancer. Clin Cancer Res 2008;14:5995–6004. [PubMed: 18829478]

Cano DA, Murcia NS, Pazour GJ, Hebrok M. Orpk mouse model of polycystic kidney disease reveals essential role of primary cilia in pancreatic tissue organization. Development 2004;131:3457–67. [PubMed: 15226261]

Cano DA, Sekine S, Hebrok M. Primary cilia deletion in pancreatic epithelial cells results in cyst formation and pancreatitis. Gastroenterology 2006;131:1856–69. [PubMed: 17123526]

Corbit KC, Aanstad P, Singla V, Norman AR, Stainier DY, Reiter JF. Vertebrate Smoothened functions at the primary cilium. Nature 2005;437:1018–21. [PubMed: 16136078]

Feldmann G, Dhara S, Fendrich V, Bedja D, Beaty R, Mullendore M, et al. Blockade of hedgehog signaling inhibits pancreatic cancer invasion and metastases: a new paradigm for combination therapy in solid cancers. Cancer Res 2007;67:2187–96. [PubMed: 17332349]

Heeschen C. J Clin Invest. 2008 ELETTERs (http://www.jci.org/eletters/view/34401).

Hermann PC, Huber SL, Herrler T, Aicher A, Ellwart JW, Guba M, et al. Distinct populations of cancer stem cells determine tumor growth and metastatic activity in human pancreatic cancer. Cell Stem Cell 2007;1:313–23. [PubMed: 18371365]

Hoffmann AC, Mori R, Vallbohmer D, Brabender J, Klein E, Drebber U, et al. High expression of HIF1a is a predictor of clinical outcome in patients with pancreatic ductal adenocarcinomas and correlated to PDGFA, VEGF, and bFGF. Neoplasia 2008;10:674–9. [PubMed: 18592007]

Hwang JM, Weng YJ, Lin JA, Bau DT, Ko FY, Tsai FJ, et al. Hypoxia-induced compensatory effect as related to Shh and HIF-1alpha in ischemia embryo rat heart. Mol Cell Biochem 2008;311:179–87. [PubMed: 18228117]

Ingham PW, McMahon AP. Hedgehog signaling in animal development: paradigms and principles. Genes Dev 2001;15:3059–87. [PubMed: 11731473]

Jemal A, Tiwari RC, Murray T, Ghafoor A, Samuels A, Ward E, et al. Cancer statistics, 2004. CA Cancer J Clin 2004;54:8–29. [PubMed: 14974761]

Kawahira H, Scheel DW, Smith SB, German MS, Hebrok M. Hedgehog signaling regulates expansion of pancreatic epithelial cells. Dev Biol 2005;280:111–21. [PubMed: 15766752]

Kayed H, Kleeff J, Osman T, Keleg S, Buchler MW, Friess H. Hedgehog signaling in the normal and diseased pancreas. Pancreas 2006;32:119–29. [PubMed: 16552330]

Lee KM, Nguyen C, Ulrich AB, Pour PM, Ouellette MM. Immortalization with telomerase of the Nestin-positive cells of the human pancreas. Biochem Biophys Res Commun 2003;301:1038–44. [PubMed: 12589817]

Li C, Heidt DG, Dalerba P, Burant CF, Zhang L, Adsay V, et al. Identification of pancreatic cancer stem cells. Cancer Res 2007;67:1030–7. [PubMed: 17283135]

Lipinski RJ, Gipp JJ, Zhang J, Doles JD, Bushman W. Unique and complimentary activities of the Gli transcription factors in Hedgehog signaling. Exp Cell Res 2006;312:1925–38. [PubMed: 16571352]

Liu MS, Yang PY, Yeh TS. Sonic hedgehog signaling pathway in pancreatic cystic neoplasms and ductal adenocarcinoma. Pancreas 2007;34:340–6. [PubMed: 17414057]

Marigo V, Davey RA, Zuo Y, Cunningham JM, Tabin CJ. Biochemical evidence that patched is the Hedgehog receptor. Nature 1996;384:176–9. [PubMed: 8906794]

McMahon AP, Ingham PW, Tabin CJ. Developmental roles and clinical significance of hedgehog signaling. Curr Top Dev Biol 2003;53:1–114. [PubMed: 12509125]

Morton JP, Mongeau ME, Klimstra DS, Morris JP, Lee YC, Kawaguchi Y, et al. Sonic hedgehog acts at multiple stages during pancreatic tumorigenesis. Proc Natl Acad Sci U S A 2007;104:5103–8. [PubMed: 17372229]

Murone M, Rosenthal A, de Sauvage FJ. Sonic hedgehog signaling by the patched-smoothened receptor complex. Curr Biol 1999;9:76–84. [PubMed: 10021362]

Nagai S, Nakamura M, Yanai K, Wada J, Akiyoshi T, Nakashima H, et al. Gli1 contributes to the invasiveness of pancreatic cancer through matrix metalloproteinase-9 activation. Cancer Sci 2008;99:1377–84. [PubMed: 18410405]

Nagase T, Nagase M, Machida M, Fujita T. Hedgehog signalling in vascular development. Angiogenesis 2008;11:71–7. [PubMed: 18301996]

Nielsen SK, Mollgard K, Clement CA, Veland IR, Awan A, Yoder BK, et al. Characterization of primary cilia and Hedgehog signaling during development of the human pancreas and in human pancreatic duct cancer cell lines. Dev Dyn 2008;237:2039–52. [PubMed: 18629868]

Odent S, Atti-Bitach T, Blayau M, Mathieu M, Aug J, Delezo de AL, et al. Expression of the Sonic hedgehog (SHH) gene during early human development and phenotypic expression of new mutations causing holoprosencephaly. Hum Mol Genet 1999;8:1683–9. [PubMed: 10441331]

Pasca di Magliano M, Hebrok M. Hedgehog signalling in cancer formation and maintenance. Nat Rev Cancer 2003;3:903–11. [PubMed: 14737121]

Pasca di Magliano M, Sekine S, Ermilov A, Ferris J, Dlugosz AA, Hebrok M. Hedgehog/Ras interactions regulate early stages of pancreatic cancer. Genes Dev 2006;20:3161–73. [PubMed: 17114586]

Pepinsky RB, Rayhorn P, Day ES, Dergay A, Williams KP, Galdes A, et al. Mapping sonic hedgehog-receptor interactions by steric interference. J Biol Chem 2000;275:10995–1001. [PubMed: 10753901]

Peralta Soler A, Knudsen KA, Jaurand MC, Johnson KR, Wheelock MJ, Klein-Szanto AJ, et al. The differential expression of N-cadherin and E-cadherin distinguishes pleural mesotheliomas from lung adenocarcinomas. Hum Pathol 1995;26:1363–9. [PubMed: 8522310]

Rohatgi R, Milenkovic L, Scott MP. Patched1 regulates hedgehog signaling at the primary cilium. Science 2007;317:372–6. [PubMed: 17641202]

Straface G, Aprahamian T, Flex A, Gaetani E, Biscetti F, Smith RC, et al. Sonic Hedgehog Regulates Angiogenesis and Myogenesis During Post-Natal Skeletal Muscle Regeneration. J Cell Mol Med. 2008

Thayer SP, di Magliano MP, Heiser PW, Nielsen CM, Roberts DJ, Lauwers GY, et al. Hedgehog is an early and late mediator of pancreatic cancer tumorigenesis. Nature 2003;425:851–6. [PubMed: 14520413]

Tian H, Callahan CA, Dupree KJ, Darbonne WC, Ahn CP, Scales SJ, et al. Hedgehog signaling is restricted to the stromal compartment during pancreatic carcinogenesis. Proc Natl Acad Sci U S A. 2009

Tsutsumida H, Swanson BJ, Singh PK, Caffrey TC, Kitajima S, Goto M, et al. RNA interference suppression of MUC1 reduces the growth rate and metastatic phenotype of human pancreatic cancer cells. Clin Cancer Res 2006;12:2976–87. [PubMed: 16707592]

Velcheti V. Hedgehog signaling is a potent regulator of angiogenesis in small cell lung cancer. Med Hypotheses 2007;69:948–9. [PubMed: 17637503]

Villavicencio EH, Walterhouse DO, Iannaccone PM. The sonic hedgehog-patched-gli pathway in human development and disease. Am J Hum Genet 2000;67:1047–54. [PubMed: 11001584]

Wahl JK 3rd, Kim YJ, Cullen JM, Johnson KR, Wheelock MJ. N-cadherincatenin complexes form prior to cleavage of the proregion and transport to the plasma membrane. J Biol Chem 2003;278:17269–76. [PubMed: 12604612]

Yauch RL, Gould SE, Scales SJ, Tang T, Tian H, Ahn CP, et al. A paracrine requirement for hedgehog signalling in cancer. Nature 2008;455:406–10. [PubMed: 18754008]

Zhang Q, Davenport JR, Croyle MJ, Haycraft CJ, Yoder BK. Disruption of IFT results in both exocrine and endocrine abnormalities in the pancreas of Tg737(orpk) mutant mice. Lab Invest 2005;85:45–64. [PubMed: 15580285]

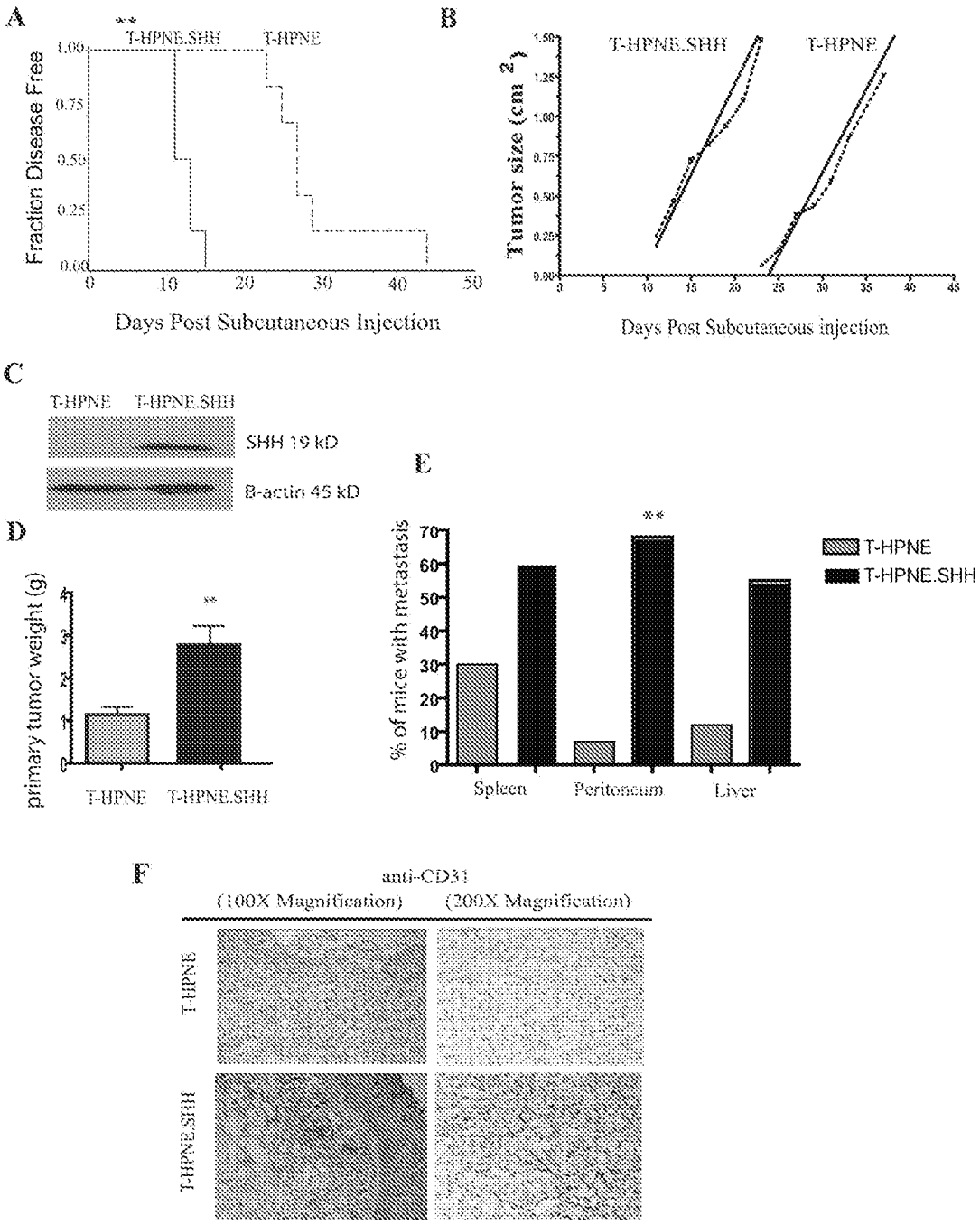

Figure 1. SHH decreased time-to-tumor progression and promoted tumor growth and metastasis in subcutaneous and orthotopic models of pancreatic cancer

A. Subcutaneous tumor growth properties in nude mice. Kaplan-Meier plot of time to tumor progression, as evidenced by % disease-free mice over time (n=5 for both groups, representative of 3 independent experiments). SHH overexpression in the T-HPNE cell line significantly decreased the time to tumor progression with an average time-to-tumor progression of 11 days in the T-HPNE+SHH cell line and an average time-to-tumor progression of 27 days with the T-HPNE cell line (**p= 0.001). Estimates of time to tumor formation were analyzed using the log-rank test.

B. Tumor growth rates. Graphical representation of tumor growth rate (volume, n=5 for both groups, representative of 3 independent experiments). Values are given in cm^3. Once tumors appeared, there were no significant differences in growth rate between transformed T-HPNE cell lines with and without SHH.
C. Western blot confirmation of expression of mature SHH in orthotopic T-HPNE tumors.
D. SHH significantly increased primary tumor weight in orthotopic tumors harvested at 46 days post tumor challenge (lower panel) (*$p < 0.01$). Bar graphs represent mean primary tumor weights (mean ± SD) (n=13).
E. SHH increased metastasis to the spleen, peritoneum (*$p < 0.01$) and liver in an orthotopic model of pancreatic cancer at 46 days post-tumor challenge. Bar graphs represent quantitative analysis of number of mice with metastatic lesions detected in the spleen, peritoneum or liver, total mice per group = 13.
F. Immunohistochemical analysis with anti-CD31 staining (brown stain) demonstrates that T-HPNE.SHH tumors have increased vascularity as compared to T.HPNE orthotopic tumors. Analysis shown at 100x magnification.

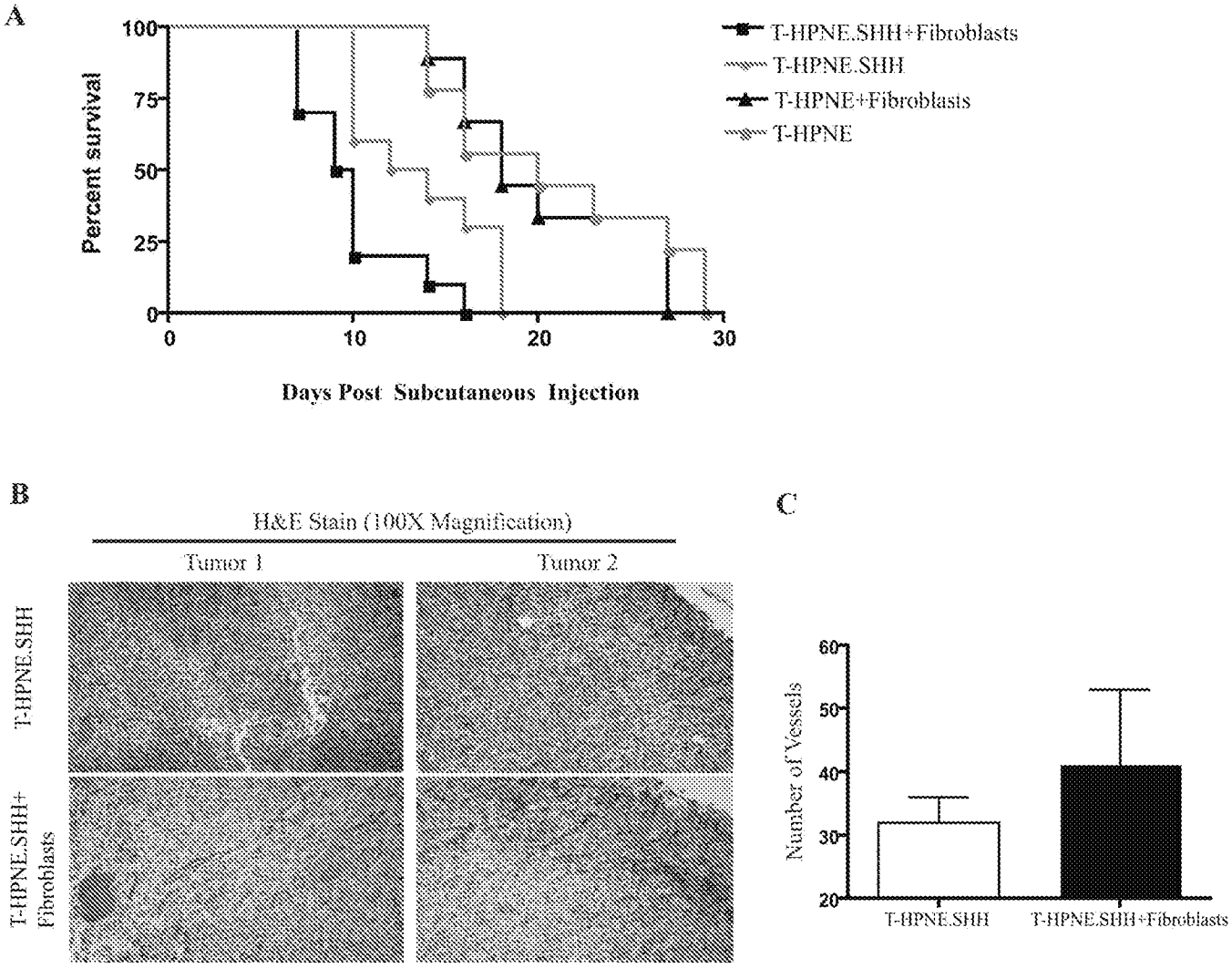

Figure 2. Co-injection of T-HPNE.SHH cells with pancreatic fibroblasts increases tumorigenesis and angiogenesis *in vivo*

A. Subcutaneous tumor growth properties in nude mice using co-cultures. Kaplan-Meier plot of time to tumor progression, as evidenced by % disease-free mice over time (n=5 for both groups, representative of 2 independent experiments). T-HPNE.SHH cells co-injected with pancreatic fibroblasts significantly decreased the time to tumor progression with an average tumor-to-tumor progression of 9 days for the T-HPNE.SHH cell line with fibroblasts compared to an average time-to-tumor progression of 12 days with the T-HPNE.SHH cell line (**p= 0.01). There was no difference observed in time-to-tumor progression between the T-HPNE cell line and the T-HPNE cell line co-cultured with pancreatic fibroblasts. Statistical analysis of time to tumor formation by the log-rank test.

B. H&E analysis of the subcutaneous tumors showing an increase in density of blood vessels (vessels containing red blood cells in this image) when the T-HPNE.SHH cells were co-injected with pancreatic fibroblasts (n=2 analyzed per group).

C. Graphical representation of morphometric analysis of the number of blood vessels per tumor section in the T-HPNE.SHH tumor and the T-HPNE.SHH tumor co-cultured with pancreatic fibroblasts. The tumors derived from the co-culture had increased angiogenesis when compared to the T-HPNE.SHH tumors.

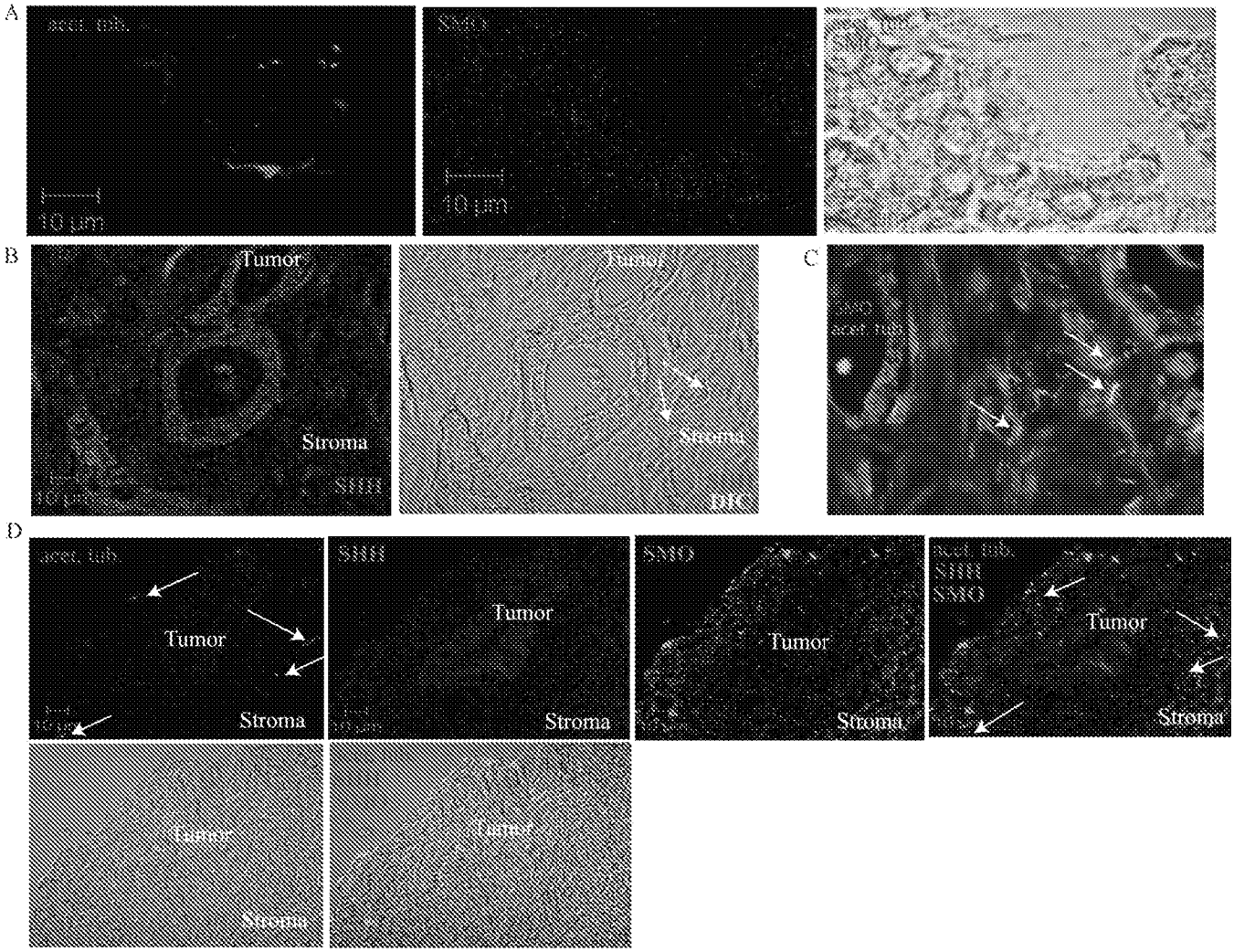

Figure 3. Stromal cells express primary cilia

A. Confocal immunofluorescence analysis of a normal mouse pancreas. Acetylated α tubulin (acet. tub.) was used to identify primary cilia (purple). SMO expression is in green. Overlay with DIC shows expression of the primary cilia on normal ductal cells of the pancreas. SMO is expressed at low levels in both acinar and ductal cells.

B. Confocal immunofluorescence analysis of a primary tumor from a patient with pancreatic cancer. SHH staining is shown in red. DIC overlay confirms SHH expression in adenocarcinoma cells and the presence of cilia in the stroma (note white arrows).

C. Immunofluorescence staining of acet. tub. (grey) and SMO (green) in a serial section of the tumor analyzed in panel **B.** Overlay confirms localization of SMO on primary cilia in stromal cells (white arrows).

D. Confocal immunofluorescence analysis of acet. tub. (purple), SHH (red) and SMO (green) in a liver metastasis from a patient with pancreatic cancer. Overlay shows primary cilia are localized to the stromal cells (white arrows). Stromal cells also show increased expression of SMO. *Analysis shown in this figure reflects staining patterns observed in 4 different patients.

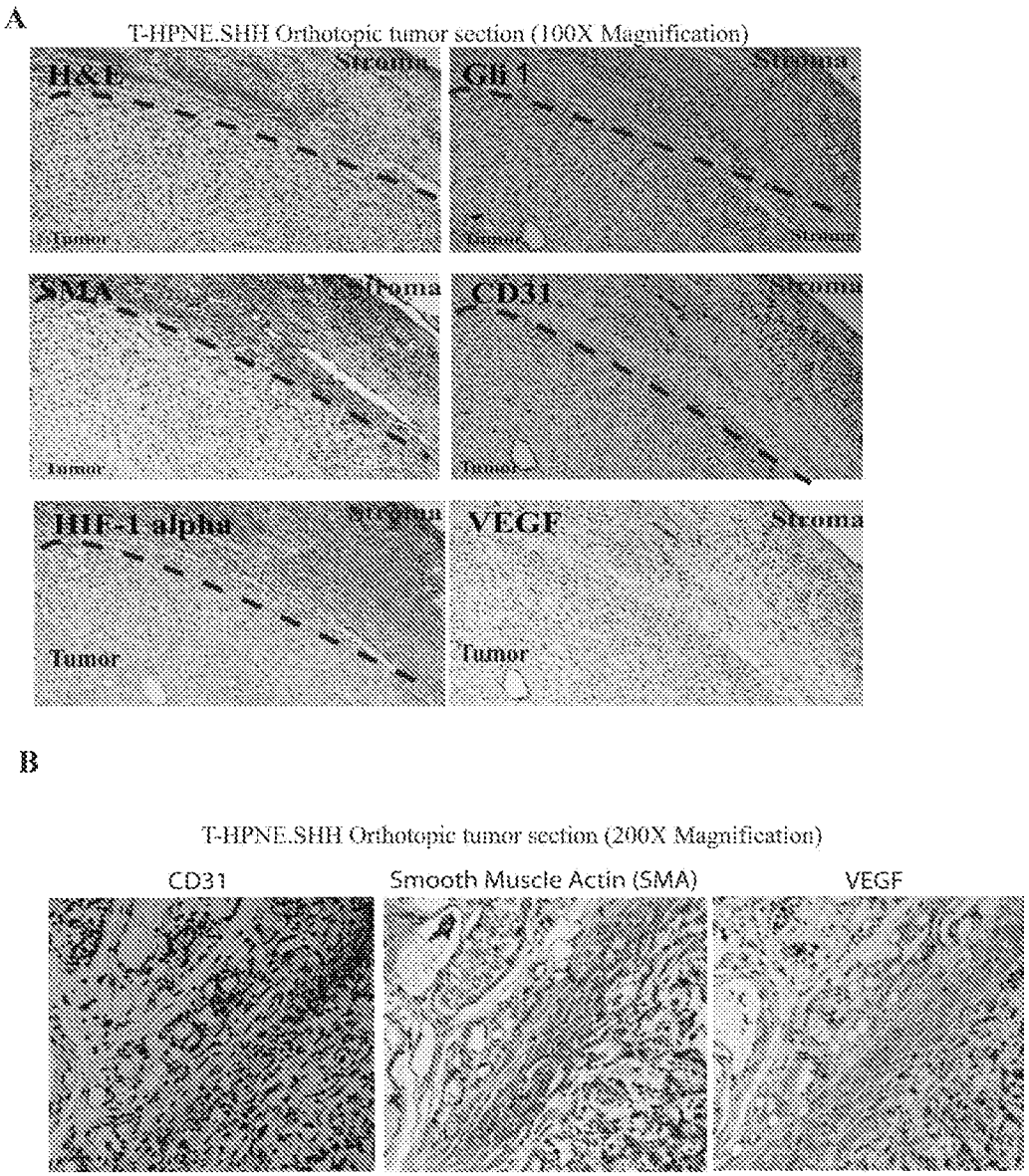

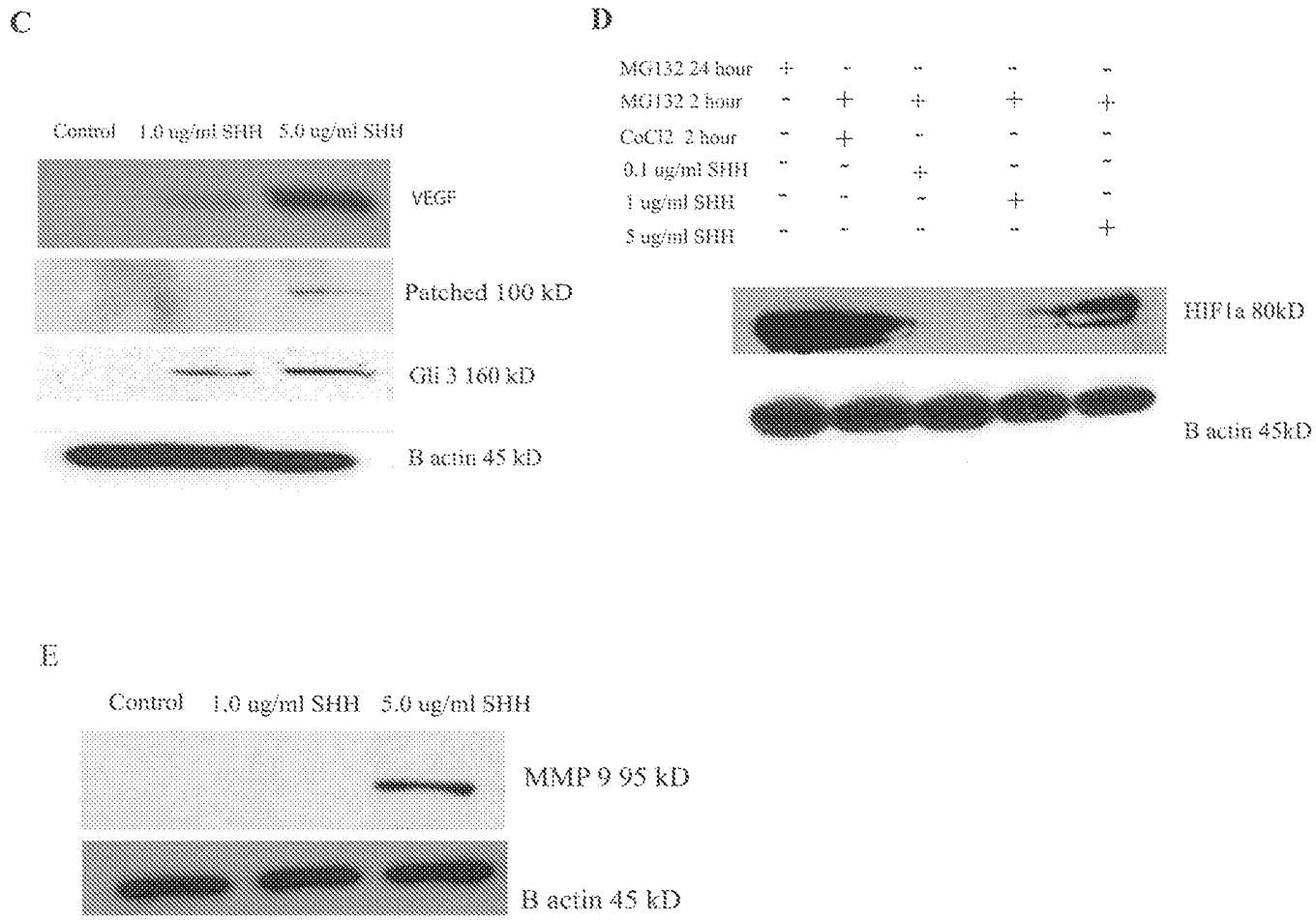

Figure 4. Downstream pathways activated in SHH stimulated pancreatic fibroblasts

A. Immunohistochemistry on orthotopic tumor sections derived from the T-HPNE.SHH cell line. Tumor-associated fibroblasts expressing SMA show expression of Gli1, VEGF and HIF1α.

B. Immunohistochemistry on orthotopic tumor sections derived from the T-HPNE.SHH cell line. SMA+ fibroblasts, along with CD31+ endothelial cells express VEGF.

C. Western blot analysis of Patched and Gli3 expression by pancreatic fibroblasts in culture. Stimulation with recombinant SHH increased Patched and Gli3 expression, indicating direct SHH pathway activation in the fibroblasts. Western blot analysis of whole cell lysates from recombinant SHH stimulated pancreatic fibroblasts, which express higher levels of VEGF in response to SHH.

D. Western blot analysis of recombinant SHH-stimulated pancreatic fibroblasts showing increased stabilization of HIF1α under normoxic conditions when stimulated with SHH. The fibroblasts were stimulated with increasing concentrations of SHH and were also stimulated with MG132 for 2 hours prior to cell lysate extraction. The HIF1α band identified by western blotting at 80kD was the same size as the band identified following treatment with $CoCl_2$.

E. Western blot analysis showing that stimulation with recombinant SHH increases the expression of MMP 9 in pancreatic fibroblasts.

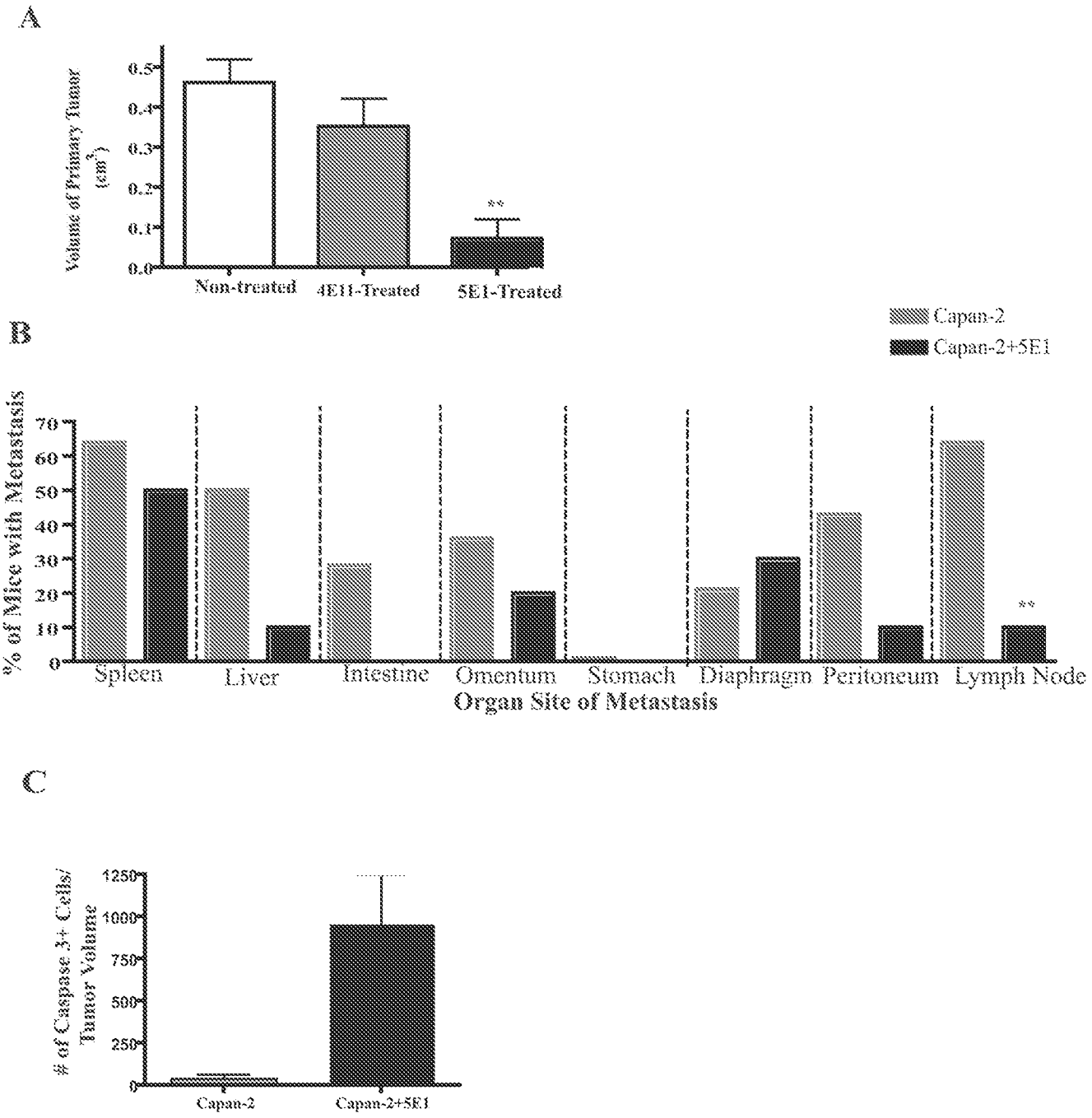

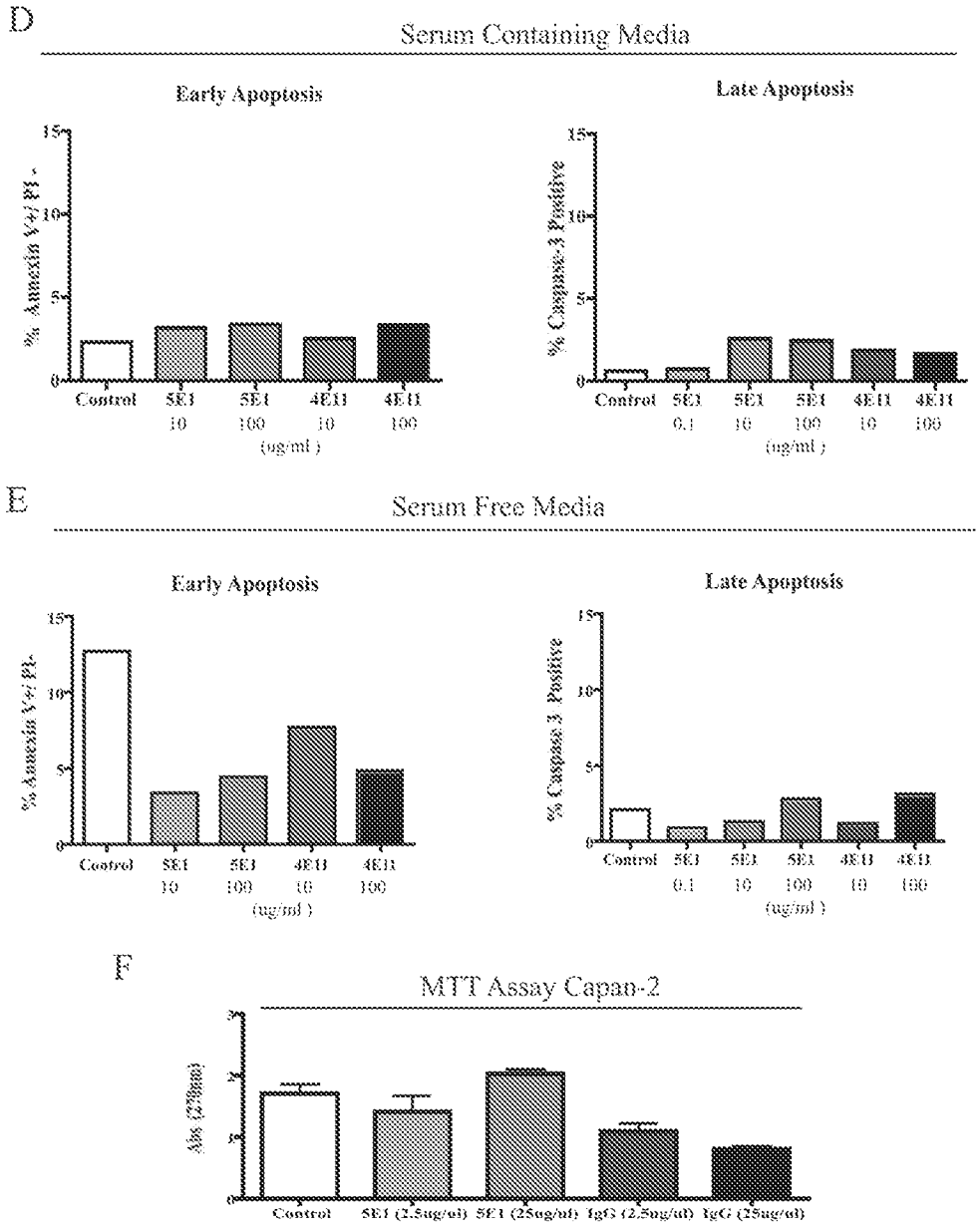

Figure 5. An SHH-neutralizing antibody decreases tumor growth, metastasis and lymphangiogeneis in an orthoptopic model of pancreatic cancer

A. Graphical representation of primary tumor volume (cm^3) in mice with Capan-2 orthotopic tumors. Average volumes are shown for untreated mice (n=15), mice that were administered an isotype control antibody (4E11) (n=5), and mice administered the SHH-neutralizing antibody, 5E1 (n=15).

B. Graphical representation of the number of mice with metastasis to different organ sites. The untreated and 5E1-treated mice were compared (n=15 each).

C. Morphometric quantification of the number of caspase 3+ cells per tumor volume in the untreated vs. 5E1-treated mice with Capan-2 tumors (n=2 per group).

D and E. 5E1 treated Capan-2 cells do not show evidence of apoptosis in serum containing media (D) or serum free (E) media. Quantification of Annexin V and caspase-3 staining by flow cytometry.

F. Treatment of Capan-2 cells *in vitro* with 5E1 does not affect proliferation rate. Graphical representation of results of MTT assays following treatment of cultures with 5E1 (anti-SHH) or control antibodies.

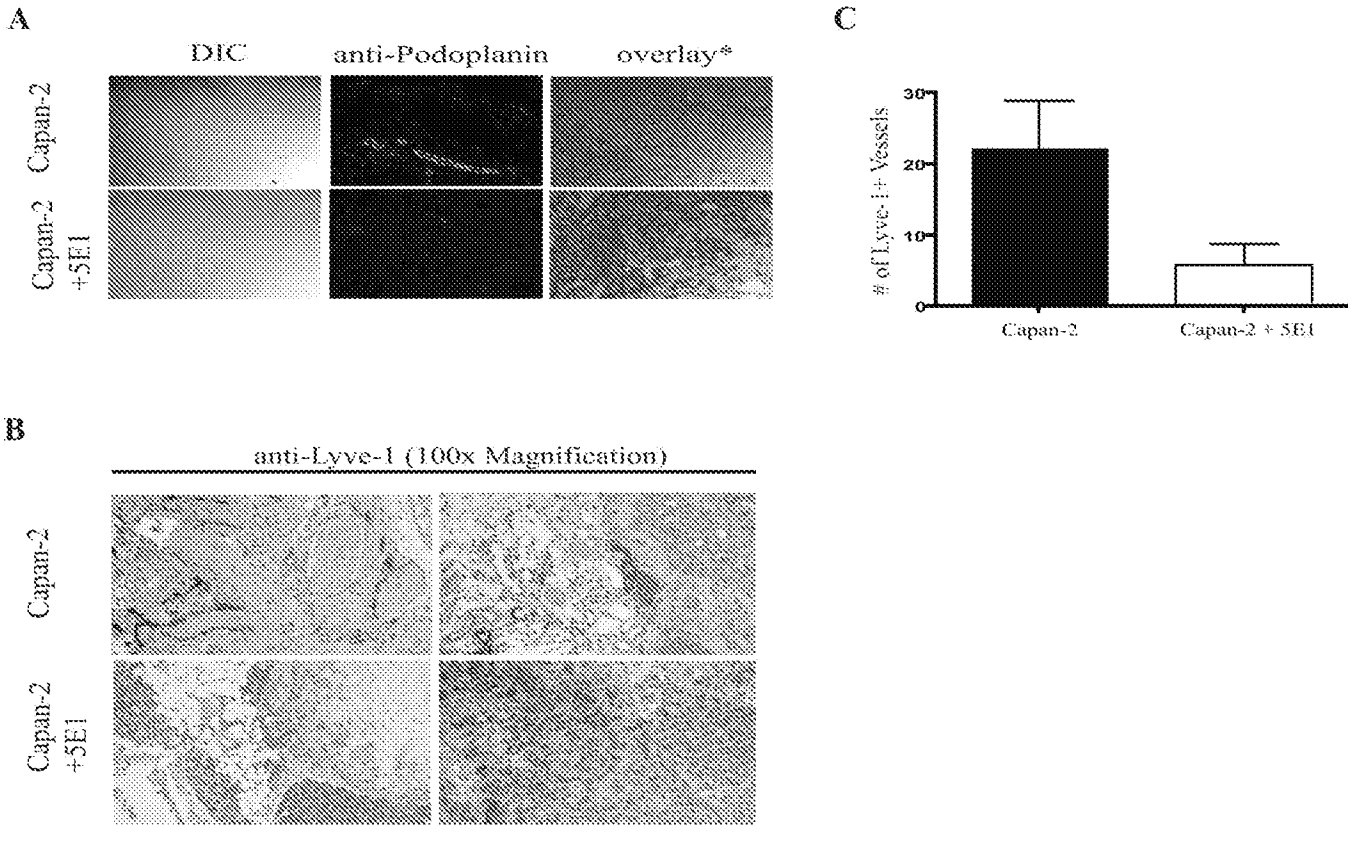

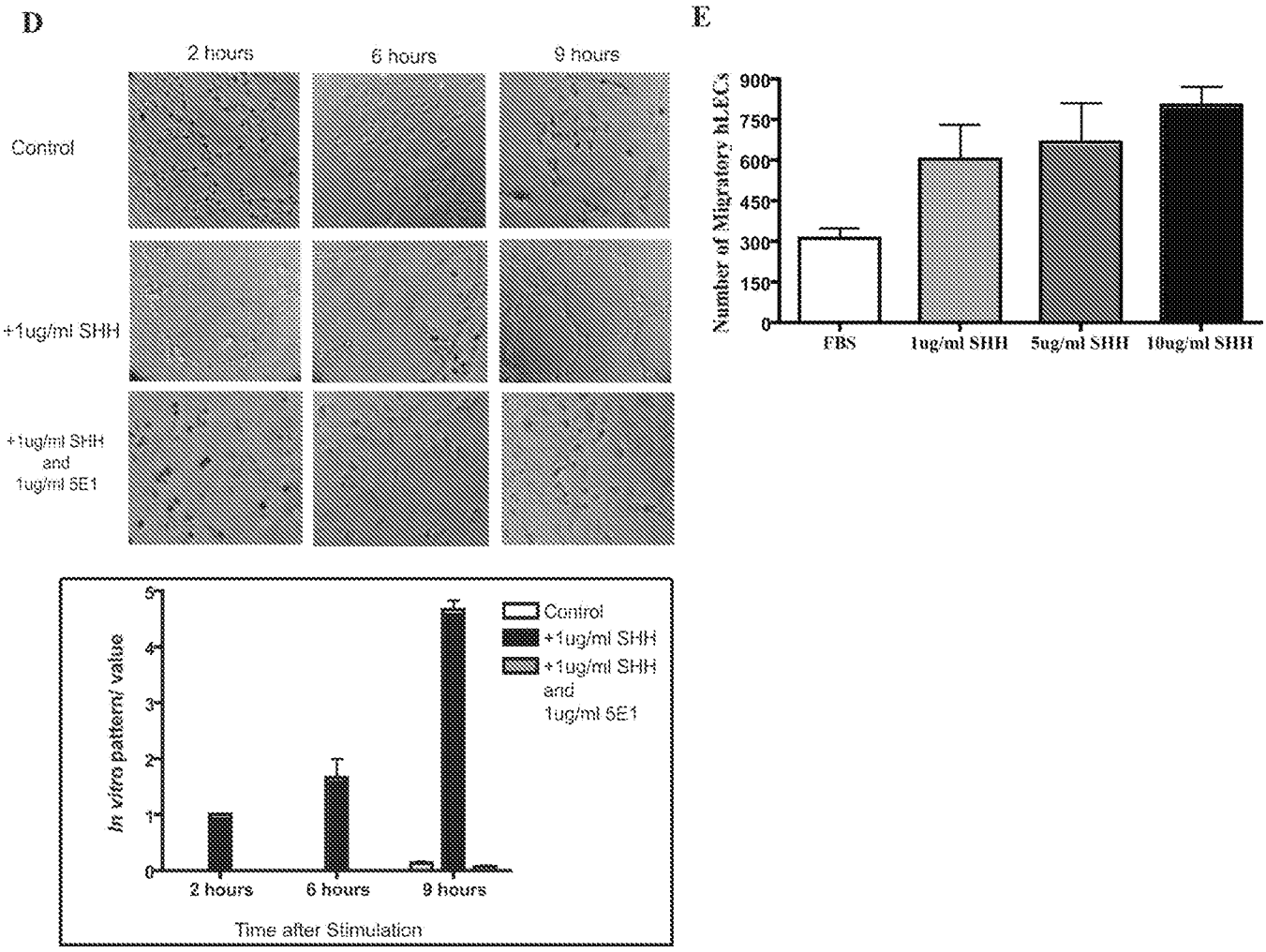

Figure 6. SHH paracrine signaling regulates lymphangiogenesis in pancreatic cancer

A. Confocal immunofluorescence analysis for the lymphatic marker, Podoplanin (green) and human ribonuclear protein staning (blue) to identify the Capan-2 tumor.

B. IHC analysis for the lymphatic marker, Lyve-1 (brown stain) in the orthotopic tumors derived from mice with either no treatment or 5E1-treatment.

C. Graphical representation of the number of Lyve-1+ vessels counted from the IHC in panel B. Treatment with 5E1 significantly decreased the number of Lyve-1+ vessels in the tumor sections (n=7 per group). Treatment with 5E1 significantly decreased the number of Lyve-1+ vessels (*p=0.01).

D. *In vitro* angiogenesis assay using the HMVEC cell line. Stimulation with recombinant SHH enhanced tube formation on matrigel. SHH enhanced the rate of endothelial cell alignment (score of 1), endothelial cell sprouting (score of 3), and the formation of complex mesh-like polygon structures *in vitro* (score of 5). Treatment with 5E1 reversed the affects of SHH.

E. Stimulation with recombinant SHH significantly increased the motility of HMVECs *in vitro* using transwell migration assays when stimulated with 10μg/ml rhSHH (*p=0.01).

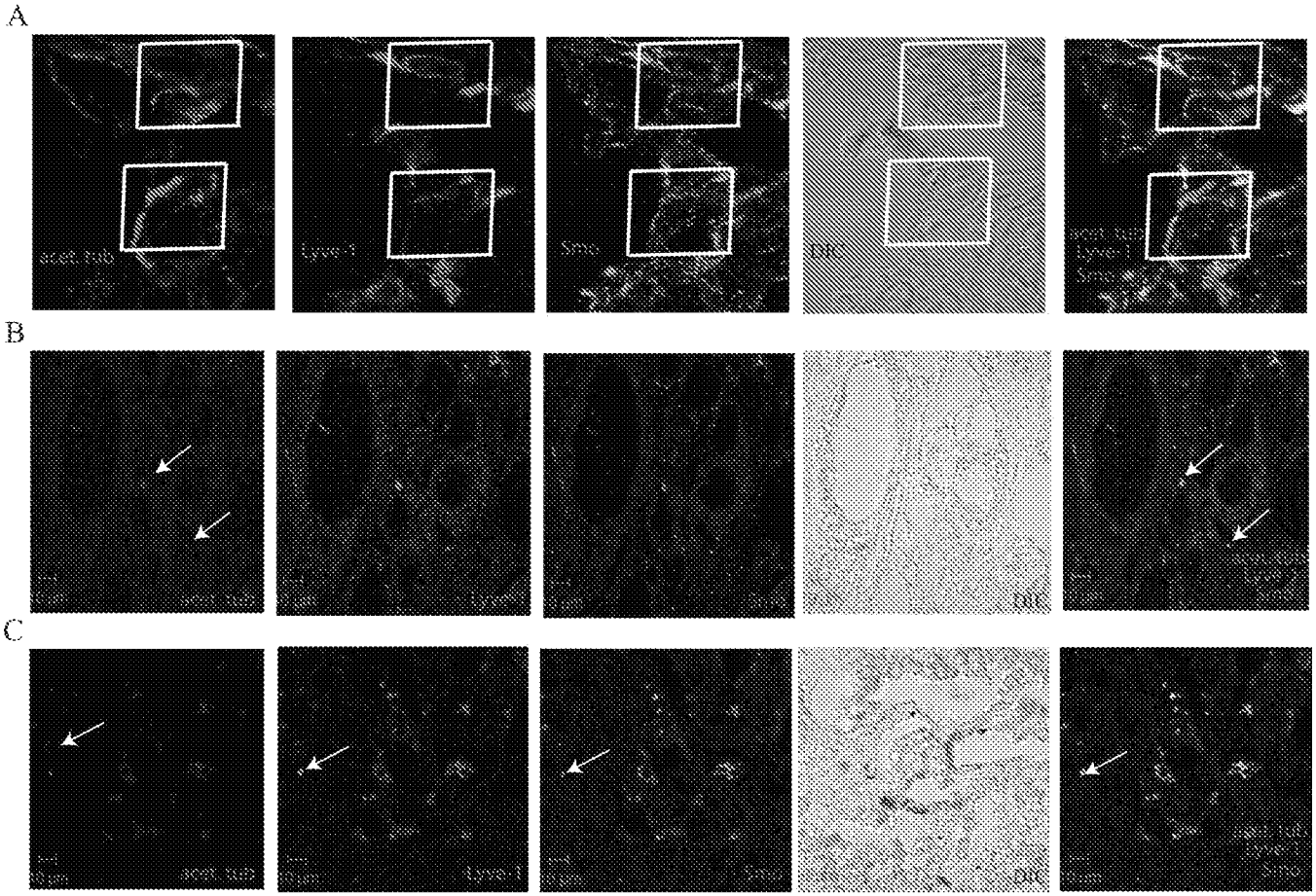

Figure 7. Primary cilia expressed on Lyve-1+ cells

A. Confocal analysis of acet. tub. (purple), Lyve-1 (red) and SMO (green) in a Capan-2 orthotopic tumor. Overlay of acet. tub. and SMO is shown on two independent Lyve-1+ cells identified in the stroma of the orthotopic tumor (white boxes).

B. Confocal analysis of acet. tub. (purple), Lyve-1 (red) and SMO (green) in a primary tumor section. Lyve-1+ vessels are expressing primary cilia and SMO is localized to the base of the cilia in identified vessels (white arrows).

C. Confocal analysis of acet. tub. (purple), Lyve-1 (red) and SMO (green) in a liver metastasis. Lyve-1+ cells are expressing primary cilia and SMO is localized to the base of the cilia in identified vessels (white arrow).